

Application of an Obstruction-Scaling Model To Diffusion of Vitamin B₁₂ and Proteins in Semidilute Alginate Solutions

Yu Zhang and Brian G. Amsden*

Department of Chemical Engineering, Queen's University, Kingston ON, Canada K7L 3N6

Received October 14, 2005; Revised Manuscript Received November 30, 2005

ABSTRACT: Pulsed field gradient nuclear magnetic resonance (PFG-NMR) was used to measure tracer diffusion coefficients of vitamin B₁₂ and globular proteins (myoglobin, β -lactoglobulin, ovalbumin, and bovine serum albumin) in semidilute alginate solutions under physiological conditions (pH 7.4, ionic strength 0.22 M). The long-time diffusion behavior can be predicted by an obstruction-scaling model, which assumes that the semidilute polymer solutions can be treated as a static network during the diffusion time scale, and the contributions of hydrodynamic interactions and electrostatic interactions to diffusion can be neglected. Arguments are given in support of these assumptions, which are expected to be valid only when the size of the probe is much larger than the polymer chain. The model was also applied to literature data of protein diffusion in flexible and inflexible polymer solutions, and it was found to be predictive. Moreover, it is demonstrated that, at equal polymer solution mesh sizes, probe diffusion is not influenced by the polymer chain flexibility.

Introduction

The diffusion of proteins in polyelectrolyte solutions not only is of great theoretical interest but also plays a fundamental and significant role in biological systems.^{1–9} A number of models have been proposed to describe this important transport phenomenon, and recently reviews were presented by Masaro and Zhu¹⁰ and Amsden.¹ These reviews indicate that a universal and predictive model is still unavailable due to the complexity of this problem.

Recently, an obstruction-scaling model was developed by Amsden to describe solute probe tracer diffusion in hydrogels^{11,12} then extended to semidilute neutral polymer solutions for which it provided good fits to literature data.¹ The motivation of the present work is to further test this model by application to the diffusion of globular proteins in polyelectrolyte solutions under physiological conditions, and to verify the assumptions of this model. Alginate was chosen as the polyelectrolyte for this study. Alginate is widely being investigated as a drug delivery and bioencapsulation material due to its biocompatibility and unique ionotropic gel-forming properties.¹³ Sodium alginate is a semiflexible polyelectrolyte, consisting of (1–4)-linked monomers of β -D-mannuronic acid and α -L-guluronic acid. The α (1–4) linkage of the guluronic acid residues introduces great steric hindrance from the carboxyl groups and the Kuhn statistical segment-length at infinite ionic strength of alginate is as high as 155 Å, which indicates a high degree of rigidity.¹⁴ The pK_a values for mannuronic unit and guluronic unit are 3.38 and 3.65, respectively.¹⁵ Hence, above pH 7, all the acid groups are ionized.

We chose to investigate globular proteins as probes because of their important roles in biological systems, and their appropriate sizes to investigate the semidilute polymer solution's structure, that is, smaller but comparable to the correlation length of semidilute polymer solutions. Small molecules (several angstroms) will not have their mobility significantly retarded by polymer chains, while larger polymer latex spheres (hundreds of nanometers), cannot reveal the microstructure of polymer

solutions.^{16,17} To our knowledge, few experiments have been done using globular protein probes spanning a range of sizes, which are good analogues to small size hard spheres under physiological conditions.

Typical experimental techniques to measure tracer diffusion in solution include dynamic light scattering (DLS), pulsed field gradient nuclear magnetic resonance (PFG-NMR), fluorescence recovery after photobleaching (FRAP), and fluorescence correlation spectroscopy (FCS). PFG-NMR was chosen over these other techniques because it is relatively simple and widely used. That is partly due to its requiring no special sample preparation, and straightforward data interpretation, which requires no model for the normal diffusion situation.^{18,19}

Review of the Theory of Polymer Solutions

Polyelectrolytes are polymers containing ionizable groups.²⁰ In a polar solvent, they can dissociate into charged polymer backbone and counterions spread in the solution. The charged nature of the polymer backbone introduces stiffness to the polymer chains in solution through Coulombic repulsion of like charges on nearby monomers. However, in solutions with high-salt concentration, this electrostatic interaction is fully screened, and the behavior of a polyelectrolyte approaches that of a neutral polymer.²¹

For polymer solutions, different polymer concentration regimes and corresponding critical concentrations have been proposed.²² At low concentrations, the polymer chains are separated from each other and are randomly oriented. As the polymer concentration increases, the solution becomes crowded and the polymer chains eventually touch each other. This is denoted as the overlap concentration, c^* . Quantitatively, the overlap concentration can be estimated from²²

$$c^* = \frac{3M}{4\pi N_A R_g^3} \quad (1)$$

where M is the molecular weight of polymer, N_A is Avogadro's constant, and R_g is the radius of gyration of a single polymer chain in solution.

* To whom correspondence should be addressed. E-mail: Amsden@chee.queensu.ca.

Above the overlap concentration, the chains form a transient network, which can be characterized using correlation length ξ , i.e., the average mesh size of the transient network.²² The correlation length can be estimated using

$$\xi = R_g(c^*/c)^\nu \quad (2)$$

where c is the polymer solution concentration and ν is a scaling coefficient, which has a value of 0.75 for a good solvent, 1 for a Θ solvent, and 0.5 for a marginal solvent.^{23,24} Equation 2 indicates that the correlation length is related to the physical properties of the polymer chain, its affinity for the solvent, and the polymer solution concentration.

Obstruction-Scaling Diffusion Model

This model has been derived elsewhere,¹ and its derivation is summarized for clarity. The model assumes that solute transport in polymer matrix can occur if an opening between the polymer chains large enough to permit its passage is produced through the random thermal movement of the polymer chains. Thus, solute diffusivity, D , is dependent on the probability of such an opening occurring. This assumption can be expressed as

$$D = D_0 \int_{r^*}^{\infty} g(r) dr \quad (3)$$

in which D_0 is the solute diffusivity in aqueous medium in the absence of polymer, $g(r) dr$ is the probability of finding openings between polymer chains that are between r and $r + dr$, and r^* is the critical radius required to allow solute passage. If the polymer solution is pictured as a random network of static straight polymer fibers of negligible width, the probability density function can be expressed as²⁵

$$g(r) = \frac{\pi r}{2R^2} \exp\left(-\frac{\pi(r/R)^2}{4}\right) \quad (4)$$

in which R is the mean radius of this distribution. The average radius of the openings between polymer chains is considered to be $\xi/2$, by assuming that the polymer chains exist in a regular cubic lattice. Inserting eq 4 into eq 3 and accounting for the finite thickness of a polymer chain produce the general expression

$$D = D_0 \exp\left[-\pi\left(\frac{R_h + r_f}{\xi + 2r_f}\right)^2\right] \quad (5)$$

in which r_s is the hydrodynamic radius of the solute probe, and r_f is the cross-section radius of the polymer chain. For polymer solutions, eq 2 can be inserted into eq 5, resulting in

$$D = D_0 \exp\left[-\pi\left(\frac{R_h + r_f}{R_g(c^*/c)^\nu + 2r_f}\right)^2\right] \quad (6)$$

Thus, if r_f , R_g , c^* , and ν are known for a given polymer in solution, eq 6 should be capable of a priori predictions of solute diffusivity. It is another objective of this paper to assess the predictive capability of the obstruction-scaling model for globular protein diffusion in polymer solutions.

Materials and Methods

Sodium alginate (ALG) (Protanal LF 10/60) was kindly donated by Pronova, Drammen, Norway. The weight-averaged molecular weight of this alginate is 126 000 and the guluronic acid content is 69%.²⁶ All other chemicals, for example bovine serum albumin

(BSA), myoglobin (MYO), ovalbumin (OVA), and β -lactoglobulin (BLG), were obtained from Sigma Aldrich, Canada, except where specified. All chemicals were used without further purification.

PFG-NMR Measurements. The principle of PFG-NMR is briefly described here. The introduction of spatially dependent magnetic fields along the z -direction (pointing in the NMR probe axial direction) during NMR experiments provides the method to label the spins of diffusants.^{18,19} A combination of spin echo²⁷ or stimulated spin echo²⁸ pulse sequences and pulsed field gradient makes it possible to measure the displacement of diffusants along the z -direction, which typically give a damping of the NMR signal intensity. Measuring diffusion is carried out by observing the attenuation of the amplitudes of specific NMR signals. The decay behavior was evaluated based on theory described elsewhere,¹⁸ and the diffusion coefficient was extracted by fitting the signal decay curve.

Appropriate amounts of protein were dissolved in deuterium oxide (Cambridge Isotope Laboratories Inc., 99.9%) containing 0.2 M sodium chloride (NaCl) and 20 mM pH 7.4 phosphate buffered saline (PBS). Then alginate was added to the protein solution and rapidly stirred at room temperature for 12 h. Protein and alginate concentrations were chosen to avoid phase separation. The resulting solution was filtered through a 0.45 μ m poly(vinylidene difluoride) syringe filter and transferred into a 5 mm NMR tube and sealed with Parafilm. Differential refractometer (Precision Instruments Co.) measurements demonstrated that there was no difference between the alginate concentration before and after filtration. The samples were measured as soon as possible after preparation to avoid protein degradation and aggregation. The lack of degradation and aggregation was confirmed via preliminary experiments that showed that 1-day storage did not change the results.

All ^1H NMR experiments were performed at 298 K using a Bruker Avance 600-MHz NMR spectrometer. A stimulated echo (STE) pulse sequence with bipolar gradient pulse pair and 3-9-19 WATERGATE¹⁹ to suppress the residual water peak was used to measure the self/tracer diffusion coefficient. The temperature in the NMR probe was first calibrated using methanol.²⁹ Field gradient calibration was accomplished using the self-diffusion coefficient of residual H_2O in D_2O at 298 K.³⁰ The half-width ($\delta/2$) of a bipolar pair was fixed at 4 ms and the diffusion time (Δ) was changed from 80 ms~150 ms to make sure the attenuation of the signals was consistently above 80%. The gradient strength (g) varied from 1 to 32 G/cm in 16 steps. A 2 ms delay was applied between gradients to complete the eddy-current relaxation.¹⁹ Each of the free induction decays (FID) was averaged over 40 scans, with 8 dummy scans, and was digitalized into 4K data points. A recycle delay of 5 s was used to allow full longitudinal relaxation ($>5T_1$, T_1 is the longitudinal relaxation time of a protein). With a consideration toward proton exchange, only the aliphatic region (typically 2–0.5 ppm) of the proteins was used to obtain diffusion coefficients.³¹

The diffusion coefficient was extracted by nonlinear curve fitting to the relationship between echo attenuation and pulsed field gradient parameters, which is given by

$$\ln\left(\frac{I}{I_0}\right) = -D[\gamma^2 g^2 \delta^2 (\Delta - \delta/3)] \quad (7)$$

where I is the area of the echo signal, I_0 is the maximum area amplitude of the echo signal, D is the diffusion coefficient, and γ is the gyromagnetic ratio of a proton.

Results and Discussion

Prior to examining the predictive ability of the model, it was first necessary to ensure that the alginate solutions examined were in the semidilute concentration regime. The z -averaged radius of gyration of alginate (LF 10/60) is 56.9 nm,²⁶ which was obtained from high-performance size-exclusion chromatography combined with multiple-angle laser scattering (HPSEC-RI-MALLS) measurement of 1 mg/mL alginate solution with

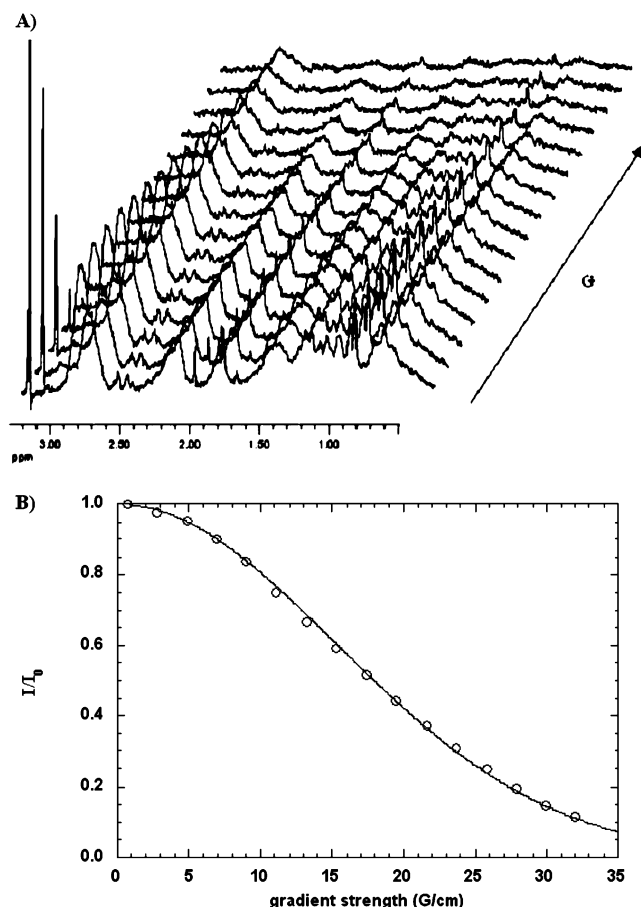


Figure 1. Example of PFG-NMR procedure for determining solute probe diffusivity. (A) Stack plot of truncated ^1H NMR spectra for the self-diffusion measurement of BSA in D_2O (4 mg/mL at 298 K). (B) Nonlinear curve fitting to extract the self-diffusion coefficient using eq 7. The value for I is the integral taken from 1 to 1.5 ppm.

an ionic strength of 0.06 M. Ionic condensation, which is calculated in terms of the Manning–Oosawa theories,^{20,32} indicates that 70% of the counterions are bound by the alginate chain. The remaining 30% of the free sodium ions will not significantly affect the ionic strength in this study. We assume that electrostatic interactions are mostly screened under this salt concentration,¹⁴ and the radius of gyration does not change significantly at an ionic strength of 0.22 M. By employment of eq 1, the overlap concentration was estimated to be 0.27 mg/mL. Therefore, it was safe to assume that the solutions with alginate concentration above 1 mg/mL are in the semidilute regime.

Diffusion Measurements. Probe Tracer Diffusion. An example of the processing of the NMR spectra to extract the diffusion coefficient is provided in Figure 1. Two common features for protein 1-D proton spectra were observed. First, signal overlaps due to overcrowding of the 1-D spectra and, second, poor sensitivity, although a large number of scans were performed. The overlap problem results from the large number of signals. The poor sensitivity problem arises from the fact that large proteins give rise to broad lines in the NMR spectra. A large line-width decreases the signal intensity and therefore also decreases the signal-to-noise ratio. As the translational long-time diffusion coefficient of proteins was being measured, the decay patterns of all the protons of the protein, except the rapidly exchanging ones in amino groups, are the same. Therefore, instead of tracking a single peak, one can track the decay pattern of a specific region to overcome the disadvantage of low

resolution and overlapping signals. The fast proton change of an amino group, from detectable N–H to undetectable N–D, makes the low field region of the spectra distorted and broadened. Therefore, the aliphatic region of protein spectra, typically 2–0.5 ppm, was chosen to extract the diffusion coefficient.³¹ The decay behavior of BSA ^1H NMR signals along with increasing of gradient field is shown in Figure 1A. The area from 1 to 1.5 ppm is integrated to yield I_0 and I for varying g . A plot of I/I_0 against g yields an exponential decay curve, which is fitted to extract the diffusion coefficient (Figure 1B). The standard errors were within 1% for a given sample. The absolute error was larger due to the uncertainty of experimental conditions, such as sample preparation, but was still within 5% percent.

It is well-known that protein diffusion is concentration dependent, and is sensitive to the pH and ionic strength of solution.^{33–39} These factors will also affect the protein monomer–dimer–oligomer equilibrium.⁴⁰ Nevertheless, in dilute solutions, when the molecules are separated and do not interact with each other, this concentration dependence is weak. In general, the characteristic volume fraction dividing the dilute and concentrated regime for proteins is 0.1.³⁸ A constant protein concentration of 4 mg/mL, which is far below this volume fraction, was therefore chosen based on preliminary experiments carried out between 1 and 10 mg/mL. The concentration after filtration might be slightly smaller due to adsorption of proteins onto the filter, but that will not affect our results. The tracer diffusion coefficients of the protein probes examined, at this apparent concentration, are listed in Table 1. The good agreement obtained with literature tracer diffusion coefficient values at infinite dilute solutions in water, indicate that at this concentration, intermolecular interactions are weak and the effect of aggregation is negligible.

Tracer Diffusion and Obstruction-Scaling Model. One complication of using globular proteins as diffusion probes is their dipolar nature. This may contribute to aggregation of the protein with itself and coacervation with a polyelectrolyte.⁴¹ The proteins chosen in this study carry the same charge, negative, with alginate. Moreover, under physiological conditions (pH 7.4, 0.2 M univalent salt without specific interaction with protein or polyelectrolyte), the electrostatic interaction between the protein probe and the polyelectrolyte would be well screened and coacervation thus avoided.

To make predictions using the obstruction-scaling model (eq 6), there are several parameters needed. The radius of the hydrated polymer was chosen to be 0.83 nm, which is the bare chain radius of 0.55 nm obtained by small-angle X-ray scattering (SAXS),⁴² plus a water layer of 0.28 nm (van der Waals radius of water is 0.14 nm).⁴³ Hydrodynamic radii of the probes were calculated using the Stokes–Einstein diffusion equation, and they are listed in Table 1. The scaling parameter for sodium alginate ν is 0.5,⁴² measured using SAXS. This indicates that the alginate solution under physiological conditions is in the marginal solvent regime, which might be due to the semiflexible nature of alginate chain.^{23,24}

Figure 2 represents the measured reduced diffusion coefficients, D/D_0 , of different probes in solutions with various alginate concentrations. Using calculated correlation lengths based on eq 2, predictions were made to test the relationships between D/D_0 and c , and between D/D_0 and R_h . These predictions are shown in Figure 2 as the solid lines. This Figure shows that, for the proteins examined, the predictions of the obstruction-scaling model are in good agreement with the experimental results. Moreover, the obstruction-scaling model

Table 1. Properties of Diffusion Probes in Aqueous Solutions (pH 7.4 and ionic strength of 0.22 M NaCl) at 298 K^a

species	M_w (g/mol)	pI	D_0 in saline (10^{11} m ² /s)	D_0 in pure water (10^{11} m ² /s)	calcd R_h (nm) ^b	lit. D_0 in pure water	ref
VB	1355	neutral	28.2	28.0	0.87	28.8	39
MYO	17 200	7.0	11.2	11.0	2.2	11.0	34
BLG	18 400	5.2	10.2	10.5	2.5	9.6	33, 35
OVA	45 000	4.7	8.1	7.7	3.0	7.9	36
BSA	66 700	4.8	7.0	6.0	3.5	6.2	37

^a Abbreviations: VB, vitamin B₁₂; MYO, myoglobin; BLG, β -lactoglobulin; OVA, ovalbumin; BSA, bovine serum albumin; pI, isoelectric point; D_0 , self-diffusion coefficient.) ^b Calculated using the Stokes–Einstein equation.

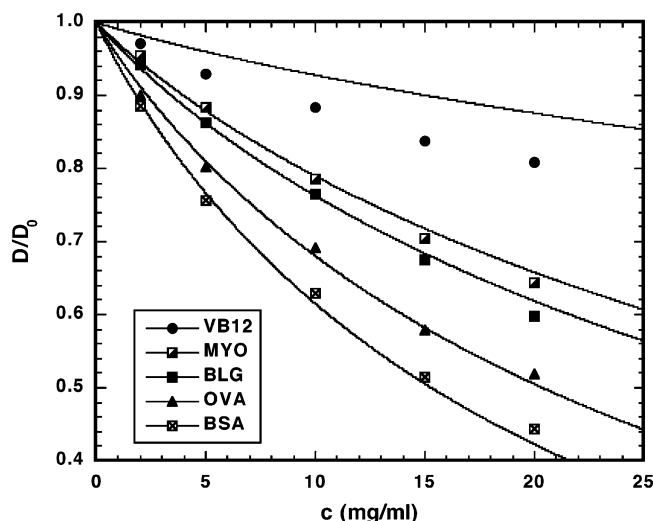


Figure 2. Reduced diffusion coefficients of various probes as a function of alginate concentration. Each data point is an average of at least two measurements, and the standard error is smaller than the marker size. Abbreviations are the same as in Table 1. The solid lines are the predicted values of the obstruction-scaling model.

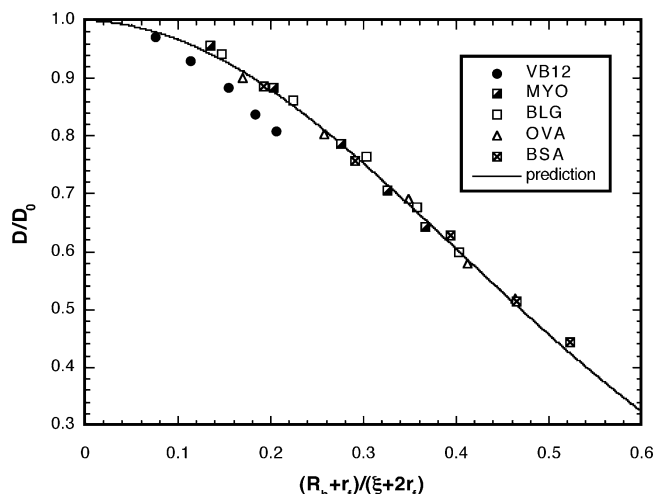


Figure 3. Comparison of the solute probes plotted in generic form as reduced diffusion coefficient vs $(R_h + r_f)/(\xi + 2r_f)$. The solid line represents the predictions of the obstruction-scaling model.

predicts that, when plotted in generic form as reduced diffusion coefficient, D/D_0 , vs $(R_h + r_f)/(\xi + 2r_f)$, the data in Figure 2 should collapse to a single line. With the exception of VB₁₂, this behavior is exhibited by the solute probes in the alginate solution (Figure 3). Similar behavior has also been demonstrated by Cheng et al.¹⁷ for spherical solute probes in poly(ethylene oxide) solution, however, they excluded the polymer chain radius. Thus, the obstruction-scaling model appears capable of a priori prediction of the diffusivity of globular proteins in polyelectrolyte solutions under physiological salt concentrations. The discrepancy of VB₁₂ with the model predictions will be

discussed along with the limiting assumptions of the model below.

Assumptions of the Obstruction-Scaling Model. The obstruction-scaling model is based on several key assumptions:

(1) Polymer chains in semidilute solution can be treated as a static network.

(2) Steric hindrance dominates the diffusive process. The contribution of hydrodynamic interactions and electrostatic interaction are negligible.

The validity of both assumptions is argued below.

a. Static Network. The argument to support the assumption of a static network is as follows.¹⁷ The lifetime of a transient mesh, τ_m , can be estimated from the viscosity and plateau modulus of a polymer solution by^{17,44}

$$\tau_m = \frac{1+k}{k} \frac{\eta_0}{G_N^0} \quad (8)$$

where G_N^0 is the plateau modulus of the shear stress relaxation of the polymer solution, k is a constant with an average value of 0.56, which is not important for our estimation, and η_0 is the zero shear rate viscosity of the polymer solution. The dependence of G_N^0 on the volume fraction of polymer is

$$G_N^0 \sim \phi^d \quad (9)$$

A value of 2.25 for d has been predicted by de Gennes.²² Matsumoto et al.⁴⁵ reported a G_N^0 value of 1×10^3 Pa for a 5 wt % solution of alginate with M_w of 2.67×10^5 mol/g and a mannuronic:guluronic (M/G) residue ratio of 0.43. They also found that G_N^0 was independent of the added salt concentration and M/G ratio. On the basis of the above statement, G_N^0 for a 10 mg/mL alginate solution should be smaller than 2.4×10^2 Pa, as the molecular weight of our alginate sample is lower. With $\eta_0(10 \text{ mg/mL}) = 30 \text{ mPa}\cdot\text{s}$,⁵² τ_m is estimated to be larger than 1.3×10^{-4} s. On the other hand, the time required for the protein probe to travel a distance of ξ requires $\tau_d \approx \xi^2/(6D)$. In our study, the diffusion coefficient of the proteins is of the order of 10^{-11} m²/s and ξ is 9.3 nm for 10 mg/mL solution, so $\tau_d \approx 1.4 \times 10^{-6}$ s. Therefore, $\tau_d \ll \tau_m$, and we can treat the mesh entanglement points as static within the diffusion time frame. The validity of this analysis can be readily verified for the other alginate concentrations.

The polymer chains in semidilute polymer solutions can be regarded as consisting of blobs of size ξ (Figure 4A). The excluded volume interaction is screened outside of a blob. Therefore, a chain can be regarded as an ideal chain consisting of monomers of size ξ . The partial chain within a blob is real, and it constantly rearranges itself without a need to move the two anchoring points (Figure 4B).⁴⁶ The dynamics follows a diffusion equation,

$$D_{\text{coop}} = \frac{kT}{6\pi\eta_s\xi_H} \quad (10)$$

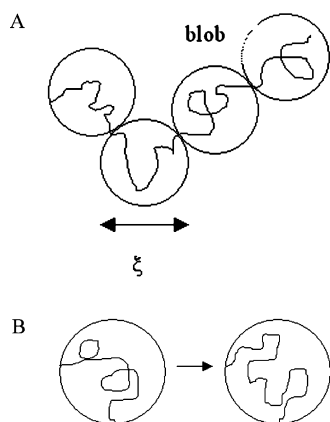


Figure 4. Polymer blob models: (A) blob model of semidilute polymer solution. (B) in-blob rearrangement of polymer chain. Adapted from ref 46.

where D_{coop} is the cooperative diffusion coefficient representing the cooperative motion of monomers within a blob. ξ_H is the dynamic correlation length, which is the counterpart of the static correlation length in eq 2, considering hydrodynamic interactions. According to de Gennes, $\xi_H = \xi$,²² while experiments have shown that ξ_H/ξ is equal or larger than unity.^{47,48} Thus, the dynamic correlation length of the alginate solution is tens of nanometers. On the basis of eq 10, the cooperative motion (rearrangements) of monomers within a blob is several times slower than the solute probes, the sizes of which are smaller than the dynamic correlation length. Therefore, within the diffusion time of the probes, we can treat the blobs as static as well. As both the entanglement points and the blobs between can both be treated as static with respect to the protein solutes, we can treat the whole transient network as static.

b. Interactions. Steric obstruction, electrostatic interactions, and hydrodynamic interactions are important influences on the diffusion of a solute probe in a polyelectrolyte solution. If there is a strong electrostatic interaction, the probe mobility will be hindered for attractive electrostatic forces and enhanced for repulsive forces. The existence of impenetrable obstacles, i.e., polymer chains, will create an increased path length for diffusion. At the same time, the movement of the chains will cause a patterned movement of the surrounding solvent molecules, which leads to a friction force on other polymer chains and the moving probes. This is called the hydrodynamic interaction. In 0.22 M physiological saline, the Debye length, which characterizes the effective range of electrostatic interactions, is 0.67 nm, which is so small that proteins can be treated as hard spheres and alginate as a semiflexible neutral polymer. Usually, electrostatic interactions are completely screened when the solution ionic strength is above 0.1 M.^{14,16,49}

It is well-known that diffusion in semidilute polymer solutions depends on the experimental time scale. At short time scales, the probe does not “feel” the surrounding chains and hydrodynamic interactions dominate, while at long time scales, both hydrodynamic interactions and obstruction effects are important.^{16,50} The experimental time scale for diffusion experiments using PFG-NMR is on the order of hundreds of milliseconds. This is several orders larger than the time needed for a probe to diffuse a distance of ξ , which is estimated to be several microseconds. Hence, the tracer diffusion coefficients we measured are long-time quantities, affected by both hydrodynamic interactions and steric obstruction. Kang et al. have proposed a theoretical approach for the diffusion of spheres in crowded suspensions of rods.¹⁶ This theory is based on a variation solution of the appropriate Smoluchowski equation

Table 2. Physical Properties of Polymers Examined

species	M_w (g/mol)	R_g (nm)	r_f (nm)	persistence length (nm)	scaling factor ν in eq 2	ref
PEO	200 000	24	0.51 ^a	0.8	0.75	17
guar	2 000 000	150	0.82 ^b	4	0.75	17
ALG	126 000	56.9	0.83	15.5	0.5	this study
DNA	115 000	50	1	56	0.5	6

^a Calculated by adding a water layer of 0.28 nm to a monomer length of 0.23 nm. ^b From ref 51.

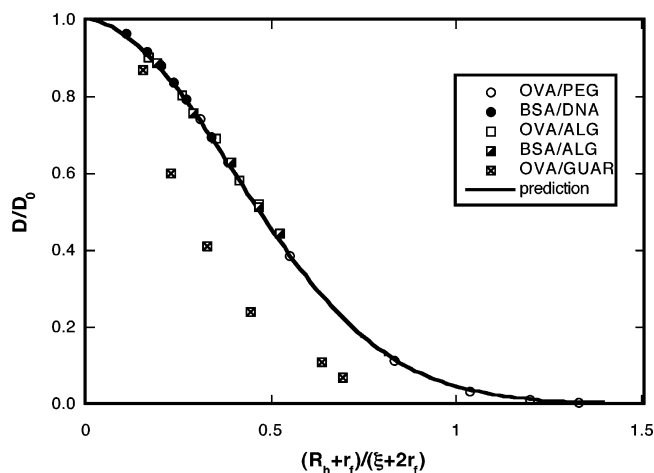


Figure 5. Comparison of the obstruction-scaling model to literature data, plotted in generic form as reduced diffusion coefficient vs $(R_h + r_f)/(\xi + 2r_f)$. The solid line represents the predictions of the obstruction-scaling model.

without hydrodynamic interactions. They found that the theoretical predictions were in accordance with experiments when the diameters of the probe sphere were relatively large compared with the rod diameter, while significant discrepancy was observed when the sphere diameter was relatively smaller. Therefore, they concluded that in the latter situation hydrodynamic interactions, which are neglected in their theory, are relatively more important compared with direct interactions. Although their theory is only valid for dilute solutions, it is commonly accepted that in semidilute solutions, hydrodynamic interactions are much more screened.^{5,16,50} In the present study, the diameters of the proteins are much larger than that of the alginate chain diameter, and on a correlation length scale, the polymer chain is rigid. Thus, we could apply Kang et al.’s theory to our systems. Therefore, the failure of the obstruction-scaling model to accurately predict the diffusivity of VB₁₂ could be attributed to the assumption of negligible hydrodynamic interactions.

Comparison To Literature Data. To further test the obstruction-scaling model, literature data of probe diffusion in other polymers with varying backbone flexibility were compared to those obtained in this study. Specifically, the data of Cheng et al.¹⁷ who examined the diffusion of ovalbumin in flexible poly(ethylene oxide) and guar solutions, and that of Wattenbarger et al.⁶ who measured diffusion of fluorescein isothiocyanate labeled BSA in more rigid DNA solutions, were used. Both studies utilized the technique of fluorescence recovery after photobleaching to measure long-time diffusion coefficients. The properties of these polymers are summarized in Table 2.

When plotted as D/D_0 vs $(R_h + r_f)/(\xi + 2r_f)$, the data collapse to a single master curve (Figure 5), with the exception of guar. The solid line in Figure 5 represents the behavior predicted by eq 5. The predicted behavior is very consistent with the data. This result indicates that the obstruction-scaling model is capable

of a priori predictions of solute diffusion in polymer solutions. Cheng et al. assumed that the scaling factor in eq 2 is 0.75 for both PEO and guar, and found that ovalbumin diffused more slowly in guar than in PEO, at the same ratio of (probe radius)/(correlation length). They attributed this discrepancy to the greater stiffness of the guar chain. However, the DNA data of Wattenbarger et al.,⁶ does not deviate from the master curve, and the persistence length of DNA is much greater (56 nm) than that of guar (4 nm) (Table 2). Moreover, as the polymer network has been demonstrated to be effectively static with respect to solute probe movement, polymer chain stiffness would not be expected to be influential. Recently, it has been reported that guar forms molecular aggregates in aqueous solution due to hydrogen bonding,⁵¹ thus, it may not be appropriate to assume that ν is 0.75 for this polymer. Further investigations into the static properties of guar might be useful in explaining this discrepancy.

Conclusions

The tracer diffusion of various proteins through physiological semidilute alginate solutions has been studied using NMR. It has been shown that, for relatively large proteins, the long-time diffusion behaviors can be successfully and a priori described using the obstruction-scaling model. For smaller probes, however, the contribution of hydrodynamic interactions should be taken into consideration. Finally, polymer chain stiffness, at equal mesh size, does not influence probe diffusion.

References and Notes

- Amsden, B. *Polymer* **2002**, *43*, 1623–1630.
- Dwyer, J. D.; Bloomfield, V. A. *Biophys. Chem.* **1995**, *57*, 55–64.
- Johansson, L.; Elvingsson, C.; Lofroth, J. E. *Macromolecules* **1991**, *24*, 6024–6029.
- Phillies, G. D. J.; Malone, C.; Ullmann, K.; Ullmann, G. S.; Rollings, J.; Yu, L. P. *Macromolecules* **1987**, *20*, 2280–2289.
- Cukier, R. I. *Macromolecules* **1984**, *17*, 252–255.
- Wattenbarger, M. R.; Bloomfield, V. A.; Bu, Z.; Russo, P. S. *Macromolecules* **1992**, *25*, 5263–5265.
- DeSmedt, S. C.; Meyvis, T. K. L.; Demeester, J.; VanOostveldt, P.; Blonk, J. C. G.; Hennink, W. E. *Macromolecules* **1997**, *30*, 4863–4870.
- Kosar, T. F.; Phillips, R. J. *AIChE J.* **1995**, *41*, 701–711.
- Busch, N. A.; Kim, T.; Bloomfield, V. A. *Macromolecules* **2000**, *33*, 5932–5937.
- Masaro, L.; Zhu, X. X. *Prog. Polym. Sci.* **1999**, *24*, 731–775.
- Amsden, B. *Macromolecules* **1999**, *32*, 874–879.
- Amsden, B. *Macromolecules* **1998**, *31*, 8382–8395.
- Gombotz, W. R.; Wee, S. F. *Adv. Drug Delivery Rev.* **1998**, *31*, 267–285.
- Smidsrod, O. *Carbohydr. Res.* **1970**, *13*, 359.
- Simsek-Ege, F. A.; Bond, G. M.; Stringer, J. J. *Appl. Polym. Sci.* **2003**, *88*, 346–351.
- Kang, K.; Gapinski, J.; Lettinga, M. P.; Buitenhuis, J.; Meier, G.; Ratajczyk, M.; Dhont, J. K. G.; Patkowski, A. *J. Chem. Phys.* **2005**, *122*.
- Cheng, Y.; Prud'homme, R. K.; Thomas, J. L. *Macromolecules* **2002**, *35*, 8111–8121.
- Price, W. S. *Concepts Magn. Res.* **1997**, *9*, 299–336.
- Price, W. S. *Concepts Magn. Res.* **1998**, *10*, 197–237.
- Oosawa, F. *Polyelectrolytes*; Marcel Dekker: New York, 1971.
- Dobrynin, A. V.; Colby, R. H.; Rubinstein, M. *Macromolecules* **1995**, *28*, 1859–1871.
- deGennes, P. G. *Scaling Concepts in Polymer Physics*; Cornell University Press: Ithaca, NY, 1979.
- Schaefer, D. W. *Polymer* **1984**, *25*, 387–394.
- Schaefer, D. W.; Joanny, J. F.; Pincus, P. *Macromolecules* **1980**, *13*, 1280–1289.
- Ogston, A. G. *Trans. Faraday Soc.* **1958**, *54*, 1754–1757.
- Donati, I.; Coslovi, A.; Gamini, A.; Skjak-Braek, G.; Vetere, A.; Campa, C.; Paoletti, S. *Biomacromolecules* **2004**, *5*, 186–196.
- Tanner, J. E.; Stejskal, E. O. *J. Chem. Phys.* **1968**, *49*, 1768.
- Tanner, J. E. *J. Chem. Phys.* **1970**, *52*, 2523.
- VanGeet, A. *Anal. Chem.* **1968**, *40*, 2227.
- Krishnan, V. V.; Thornton, K. H.; Cosman, M. *Chem. Phys. Lett.* **1999**, *302*, 317–323.
- Price, W. S.; Nara, M.; Arata, Y. *Biophys. Chem.* **1997**, *65*, 179–187.
- Manning, G. S. *J. Chem. Phys.* **1969**, *51*, 924.
- Le Bon, C.; Nicolai, T.; Kuil, M. E.; Hollander, J. G. *J. Phys. Chem. B* **1999**, *103*, 10294–10299.
- Riveros-Moreno, V.; Wittenberg, J. B. *J. Biol. Chem.* **1972**, *247*, 895.
- Beretta, S.; Chirico, G.; Baldini, G. *Macromolecules* **2000**, *33*, 8663–8670.
- Gibbs, S. J.; Chu, A. S.; Lightfoot, E. N.; Root, T. W. *J. Phys. Chem.* **1991**, *95*, 467–471.
- Meechai, N.; Jamieson, A. M.; Blackwell, J. J. *Colloid Interface Sci.* **1999**, *218*, 167–175.
- Nesmelova, I. V.; Skirda, V. D.; Fedotov, V. D. *Biopolymers* **2002**, *63*, 132–140.
- Shin, H. S.; Kim, S. Y.; Lee, Y. M.; Lee, K. H.; Kim, S. J.; Rogers, C. E. *J. Appl. Polym. Sci.* **1998**, *69*, 479–486.
- Price, W. S.; Tsuchiya, F.; Arata, Y. *J. Am. Chem. Soc.* **1999**, *121*, 11503–11512.
- Wang, Y. F.; Gao, J. Y.; Dubin, P. L. *Biotechnol. Prog.* **1996**, *12*, 356–362.
- Wang, Z. Y.; White, J. W.; Konno, M.; Saito, S.; Nozawa, T. *Biopolymers* **1995**, *35*, 227–238.
- Halle, B.; Davidovic, M. *Proc. Natl. Acad. Sci. U.S.A.* **2003**, *100*, 12135–12140.
- Baumgaertel, M.; Schausberger, A.; Winter, H. H. *Rheol. Acta* **1990**, *29*, 400–408.
- Matsumoto, T.; Mashiko, K. *Biopolymers* **1990**, *29*, 1707–1713.
- Teraoka, I. *Polymer Solutions: An Introduction to Physical Properties*; John Wiley & Sons: New York, 2002.
- Numasawa, N.; Kuwamoto, K.; Nose, T. *Macromolecules* **1986**, *19*, 2593–2601.
- Szydlowski, J.; Van Hook, W. A. *Macromolecules* **1998**, *31*, 3266–3274.
- Desmedt, S. C.; Lauwers, A.; Demeester, J.; Engelborghs, Y.; Demey, G.; Du, M. *Macromolecules* **1994**, *27*, 141–146.
- Koenderink, G. H.; Sacanna, S.; Aarts, D.; Philipse, A. P. *Phys. Rev. E* **2004**, *69*.
- Gittings, M. R.; Cipelletti, L.; Trappe, V.; Weitz, D. A.; In, M.; Marques, C. J. *Phys. Chem. B* **2000**, *104*, 4381–4386.
- The viscosities of protein free alginate solutions under physiological conditions were measured at 296 K on a rotational rheometer (AR2000, TA Instruments Inc., Houston, TX), using a cone-and-plate geometry with a diameter of 60 mm, cone angle of 1°, and gap of 30 mm. The solutions showed Newtonian behavior within the range of shear rate applied (below 10 rad/s) and zero-shear viscosities were obtained by extrapolating.

MA0522357